Fibronectin promotes elastin deposition, elasticity and mechanical strength in cellularised collagen-based scaffolds

Daniele Pezzoli [a], Joseph Di Paolo [b], Heena Kumra [b], Giulia Fois [a, c], Gabriele Candiani [c], Dieter P. Reinhardt [b, **, 1], Diego Mantovani [a, *, 1]

[a] Laboratory for Biomaterials and Bioengineering, Canada Research Chair I in Biomaterials and Bioengineering for the Innovation in Surgery, Department of Min-Met-Materials Engineering, Research Center of CHU de Quebec, Division of Regenerative Medicine, Laval University, Quebec City, QC G1V 0A6, Canada [b] Canada Research Chair I in Cell-Matrix Biology, Faculty of Medicine, Department of Anatomy and Cell Biology, and Faculty of Dentistry McGill University, Montreal, QC H3A 0C7, Canada
[c] Department of Chemistry, Materials and Chemical Engineering "Giulio Natta", Politecnico di Milano, Milan, 20131, Italy

One of the tightest bottlenecks in vascular tissue engineering (vTE) is the lack of strength and elasticity of engineered vascular wall models caused by limited elastic fiber deposition. In this study, flat and tubular collagen gel-based scaffolds were cellularised with vascular smooth muscle cells (SMCs) and supple-mented with human plasma fibronectin (FN), a known master organizer of several extracellular matrix (ECM) fiber systems. The consequences of FN on construct maturation was investigated in terms of geometrical contraction, viscoelastic mechanical properties and deposition of core elastic fiber proteins. FN was retained in the constructs and promoted deposition of elastin by SMCs as well as of several proteins required for elastogenesis such as fibrillin-1, lysyl oxidase, fibulin-4 and latent TGF-β binding protein-4. Notably, gel contraction, tensile equilibrium elastic modulus and elasticity were strongly improved in tubular engineered tissues, approaching the behaviour of native arteries. In conclusion, this study demonstrates that FN exerts pivotal roles in directing SMC-mediated remodeling of scaffolds toward the production of a physiological-like, elastin-containing ECM with excellent mechanical properties. The developed FN-supplemented systems are promising for tissue engineering applications where the generation of mature elastic tissue is desired and represent valuable advanced *in vitro* models to investigate elastogenesis.

Keywords:
Collagen gel
Fibronectin
Vascular tissue engineering
Elastic fibers
Smooth muscle cells
Mechanical properties

1. Introduction

Vascular diseases, in particular coronary artery diseases (CAD) are one of the leading causes of death in the Western society. An estimated 15.5 million Americans above the age of 20 suffer from CAD [1], and this number is predicted to strongly increase owing to the rapid growth of the elderly demographic of the population [2]. One of the most pressing clinical problems is the need for small diameter vascular grafts for coronary artery bypass surgery [3]. Tissue engineered blood vessels (TEBVs) are promising biological arterial substitutes that can serve as alternatives to autologous grafts such as internal mammary artery and saphenous vein grafts. However, many approaches did not yet translate into clinical applications. Vascular tissue engineering (vTE) approaches can be immediately impactful for the development of viable *in vitro* vascular wall models alternative to *in vivo* tests, to study the physiology and pathology of vascular tissue and for drug development [4,5].

The use of collagen type I gels (hereinafter called collagen gels) as scaffolds for vTE has a number of benefits: i) collagen type I is one of the main components of the extracellular matrix (ECM) of native vascular tissues; ii) it is abundantly available and can be readily purified from various species [6]; iii) it is non-antigenic and biocompatible; iv) collagen gels can be directly and uniformly seeded with cells during the fabrication process; and v) the collagen network can be actively remodeled by vascular smooth muscle cells (vSMCs) [7]. Since the first attempt to generate TEBVs using bovine aortic vSMCs and collagen gels as scaffolds [8], several

* Corresponding author.
** Corresponding author.
E-*mail addresses:* dieter.reinhardt@mcgill.ca (D.P. Reinhardt), diego.mantovani@gmn.ulaval.ca (D. Mantovani).
[1] co-last and co-corresponding authors.

Published Journal Article available at: https://doi.org/10.1016/j.biomaterials.2018.07.013

collagen-based tissue models and bioreactor systems to promote their dynamic maturation have been developed [9–15], and the collagen gel formulation and processing have been optimized in order to obtain enhanced mechanical properties [16–19]. However, two major challenges impede the development of physiologically relevant *in vitro* vascular wall models: (i) the relatively weak mechanical properties, and (ii) the need for the deposition and organization of an ECM that closely resembles the *in vivo* situation, especially with respect to the presence of elastic fibers and their critical physiological functions.

Elastic fibers and elastic lamellae are protein supra-structures deposited in blood vessel walls and other elastic tissues during development and early postnatal life [20]. They confer elasticity to the tissue and play key biological roles in the physiology of arteries [21]. Elastic fibers and lamellae are principally composed of a cross-linked elastin core surrounded by a mantle of fibrillin (FBN)-1-rich microfibrils required for the initial deposition and processing of tropoelastin (TE), the precursor of elastin [22]. The assembly of elastic fibers and lamellae is a highly hierarchical molecular process starting with the assembly of fibronectin (FN) which is deposited early in tissues and dependent on cell surface integrins receptors [23]. Assembled FN fibers are essential for the formation of FBN-1-containing beaded microfibrils [24,25], as well as for other ECM fiber systems including collagen I and III [26]. TE is deposited onto microfibrils with the help of several accessory proteins including fibulin (FBLN)-4 and FBLN-5, as well as latent TGF-β binding protein (LTBP)-4 [27,28]. Lysyl oxidase (LOX) and LOX-like 1 enzymes promote cross-linking of the nascent elastic fibers critical for mechanical stability and proper function [29,30]. While this fine-tuned hierarchical process of elastogenesis is required for the proper generation and function of TEBVs, it is difficult to be reproduced *in vitro* and is typically reduced in engineered tissues [31]. Furthermore, several of these elastogenic molecules regulate SMC phenotypes and function. For example, FN can strongly influence the behaviour of SMCs within 3D matrices [32], especially pro-moting the SMC synthetic phenotype [33]. On the other hand, elastin regulates proliferation and organization of vSMCs [34].

The appropriate incorporation of elastin and elastic fibers in the scaffold material would effectively address several of the biological and mechanical issues in the development of viable TEBVs. However, low production of the elastic fiber precursor TE by essentially all cell types used, its delicately orchestrated assembly process, and the large size and insolubility of mature elastic fibers make mature elastin incorporation challenging and often incompatible with many material processing techniques [35]. Several attempts have been made to promote elastogenesis in engineered tissues by means of both biochemical and mechanical stimuli, but with relatively unsatisfactory results, especially in short term approaches (up to one week of culture). In 2003, Long and Tranquillo demonstrated the deposition of FBN-1 and TE by neonatal rat aortic SMCs after 4 weeks of culture in fibrin gels, but not in collagen gels [36]. More recently, Venkataraman et al. have shown that cyclic strain combined with elastogenic factors improved deposition of elastin compared to static controls after long term (3 weeks) culture in tubular collagen gels cellularised with adult human aortic SMCs [37]. Similar results were obtained by Lee and colleagues using a poly (glycerol sebacate) scaffold with adult baboon carotid artery SMCs [38]. Elastogenesis has also been demonstrated by Hinderer et al. in short term cultures (6 days) in an electrospun fibrous 3D polymer scaffold upon dynamic maturation in a fluid-flow bioreactor [39]. However, a systematic up-scaling of that system is necessary to obtain tissues of clinically relevant size, with the associated challenge of uniform cell seeding and colonization of a thick electrospun scaffold [39].

The main hypothesis of this work is that the addition of soluble FN to cellularised collagen gels promotes their maturation into vascular wall models. Specifically, this research aimed at elucidating the influence of FN on the response of SMCs within the collagen gels, focusing on the mechanical properties and elastic fiber synthesis and deposition. Results demonstrate that the combination of collagen type I and FN, by providing an optimal 3D microenvironment with appropriate biochemical behaviour, stimulates SMCs activity for the production of engineered tissues with an *in vivo*-like elastic ECM and enhanced mechanical properties. These results highlight the key role of exogenous FN in the rapid maturation of cellularised collagen gel-based constructs.

2. Materials and methods

2.1. Cell isolation and culture

Primary porcine aortic SMCs (PAoSMCs) were derived from the tunica media of healthy, fibrous plaque-free porcine arteries. PAoSMCs were isolated from 1 cm wide aortic rings obtained from segments of the aorta of adult pigs [40]. Aortic segments were collected in phosphate-buffered saline (PBS), placed in Dulbecco's Modified Eagle's Medium (DMEM, Life Technologies) supplemented with 1% penicillin/streptomycin solution (100 U/mL penicillin, 0.1 mg/mL streptomycin; Sigma) and then dissected. The adventitial tissue and the first outer third portion of the tunica media were carefully removed and the resulting rings were cut into small pieces of approximately 1 × 5 mm, and placed in a petri dish containing DMEM supplemented with 10% fetal bovine serum (FBS; Life Technologies) and 1% penicillin/streptomycin solution (hereafter referred to as complete medium) that was changed every 2–3 days. Once a sufficient amount of SMCs migrated onto the surface of the petri dish, the explants were removed. The protocol for the isolation of PAoSMCs was approved by the Ethics Committee of CHU de Québec Research Centre. For all the experiments cells were used at a passage between 6 and 10.

2.2. Preparation of cellularised collagen gels

Type I collagen was extracted from rat tail tendons, solubilized in 0.02 N acetic acid at a concentration of 4 mg/mL and sterilized by multiple cycles of dialysis in 1% chloroform and 0.02 N acetic acid as previously described [6]. Cellularised collagen gels were prepared as previously described [41]. Briefly, 2 parts of sterile collagen so-lution were mixed with 1 part of buffer solution (3.5-fold concen-trated DMEM supplemented with 60 mM NaOH and 10 mM HEPES) and 1 part of cell suspension (2×10^6 cells/mL in complete me-dium) to obtain a final cell density of 5×10^5 cells/mL, a collagen concentration of 2 g/L and a pH of 7.2. Then, an aqueous solution containing different concentrations (5, 2.5, 1.25 and 0.625 g/L) of human plasma FN (Advanced Biomatrix) was added to gels (1:50 vol ratio) to obtain FN-loaded gels.

For the preparation of disk-shaped samples, the collagen-cell suspension was immediately poured into 24-well plates (0.5 mL/well) and incubated for 1 h at room temperature (r.t.) to allow sample gelation. Each gel was gently detached from the wall and the bottom of the well with a microspatula, 0.5 mL of fresh complete medium were added, and the constructs were incubated in a humidified atmosphere of 5% CO_2 at 37 °C for 1, 3 or 7 days. The medium was changed every second day.

For the preparation of tubular samples, 2 mL of collagen-cell suspension was poured in *ad hoc* made sterile tubular moulds composed of a central cylindrical polypropylene mandrel with a diameter of 3.8 mm, of a tubular polypropylene mould with an internal diameter of 9 mm, and two gaskets. Samples were

incubated for 1 h at r.t., then the external mould was removed and the mandrel, surrounded by the collagen tube, was placed in a sterile tube containing complete medium. Constructs were then cultured as described above.

Cell viability was evaluated by Alamar Blue assay according to the manufacturer's guidelines. Briefly, samples were incubated in complete medium containing resazurin dye for 6 h under standard culture conditions. The fluorescence of the medium ($\lambda_{ex} = 560$ nm; $\lambda_{em} = 590$ nm) was then measured using a SpectraMax i3x microplate reader (Molecular Devices).

2.3. Disk-shaped collagen gels contraction and mechanical characterization

Disk-shaped collagen gels were imaged using a flatbed scanner (Microtek Inc) and the surface area was measured using ImageJ (http://rsb.info.nih.gov/ij) [42]. Gel contraction was calculated at each time point as the ratio between the area of the sample and the area of the well, corresponding to the initial surface of the gel.

The characterization of the viscoelastic properties of disk shaped cellularised collagen gels under compression was performed by unconfined compression tests using a Biomomentum Mach 1 testing apparatus equipped with a 25 mm compression plate mounted on a 150 gf load cell and of a testing chamber allowing to perform the tests in a PBS bath. The thickness of the disks was measured by the instrument and it was always between 1 and 1.5 mm. Multiple progressive stress-relaxation cycles were applied, consisting of compression ramps of 0.1 mm at 0.02 mm/s followed by a relaxation time of 600 s at constant strain during which the stress decay was measured. At least 50% deformation was reached for each sample. Samples were immersed in PBS throughout the test period. In order to relate the stress-relaxation process to the viscoelastic parameters of the construct, the Maxwell-Wiechert model with two Maxwell elements, previously used to describe the decay of stress as a function of time in collagen gels [43], was adopted and model parameters were fit against experimental data by least squares fitting using MATLAB (MathWorks).

2.4. Tubular collagen gel contraction and mechanical characterization

The thickness of cellularised collagen constructs was assessed by measuring the external diameter of the tubular samples still mounted on their mandrel with a scanning laser interferometer (Series 183B, LaserMike 136, NDC Technologies), while the length of the constructs was measured using a calliper.

The characterization of the viscoelastic properties of cellularised collagen gels by circumferential stress-relaxation tests (ring tests) was performed using an Instron ElectroPuls E1000 system (Instron Corporation) equipped with a 5 N load cell and *ad hoc* made grips. Constructs were carefully removed from the mandrel and samples of 6 mm length were cut with a scalpel from the central part of the tube. Ring-shaped samples (internal diameter 3.8 mm) were mounted on the grips, immersed in a PBS bath at 37 °C and stretched to a 5% pre-strain. No mechanical preconditioning was performed prior to the test according to established procedures [43]. After 10 min, 5 progressive stress-relaxation cycles were applied, consisting of 10% strain ramps at 5%/s strain rate followed by a relaxation time of 600 s at constant strain during which the stress decay was measured. 50% deformation was reached for each sample at the end of the test. In order to relate the stress-relaxation process to the viscoelastic parameters of the construct and to estimate equilibrium residual stresses, the Maxwell-Wiechert model with two Maxwell elements was adopted [43].

2.5. Scanning electron microscopy (SEM)

Cellularised collagen gel samples were washed in PBS for 10 min, rinsed in 0.1 M cacodylate pH 7.4 and fixed with 2.5% glutaraldehyde in 0.1 M cacodylate, pH 7.4 for 2 h. The samples were rinsed three times with cacodylate buffer and dehydrated through sequential immersion in a graded series of increasing ethanol concentrations (50%, 70%, 95% and 100%). Samples were then transferred to a critical point drying system (Polaron CPD 7501, VG Microtech) to remove ethanol, and sputter-coated with gold-palladium. Images were captured on a FEI Quanta 250 apparatus in high-vacuum mode, using an Everhart−Thornley Detector (ETD).

2.6. Tissue and cell staining procedures

After 1, 3 or 7 days of static culture, collagen gel constructs were rinsed with PBS and fixed in 3.7% formaldehyde for 20 min at r.t., embedded in paraffin, and cut in 4 μm or 10 μm sections.

For histochemical evaluation, 10 μm sections were deparaffinised in toluene and rehydrated in graded solutions of ethanol in water, incubated overnight in Bouin solution and stained by a modified Masson's trichrome procedure (Weigert's iron hematoxylin solution, acid fuchsin and xylidine ponceau solution, and light green SF yellowish solution).

For the immunohistochemical evaluation of ECM proteins, deparaffinised 4 μm sections were rehydrated using the Dako Envision + System-HRP (AEC) immunohistochemistry kit (Dako). Heat-induced, acid, and proteinase K-mediated methods were used for antigen retrieval. Sections were stained using anti-human FN (Sigma; F3648), anti-human TE (Elastin Products Company; PR398), anti-human cellular FN (Abcam; ab6328), anti-human lysyl oxidase (Novus Biologicals; NB100-2527), anti-human latent TGF-β binding protein 4 (produced in the lab), anti-human fibulin-4 and fibulin-5 [44], anti-human FBN-1 and FBN-2 [45] antibodies. A minimum of two independent experiments were performed.

For immunofluorescence analysis, adult porcine aortic smooth muscle cells were seeded in 8-well chamber slides (20,000 per well) with DMEM (Wisent Inc.) containing 10% fetal bovine serum, 100 μg/ml penicillin/streptomycin, and 2 mM glutamine. Half of the wells were supplemented with 0.05 mg/mL human plasma FN (Millipore). It is important to note that fetal bovine serum contains FN at a concentration of 0.03 mg/mL [46]. With 10% v/v serum in the medium, the final concentration of this serum-derived FN is 0.003 mg/mL, which is negligible compared to 0.05 mg/mL of exogenous human plasma FN added to the medium. The cells were fixed with 70:30 (v/v) methanol:acetone mixture 3 or 7 days after seeding and stained using the same antibodies as described above. Secondary antibody staining was performed using Cy3-goat anti-mouse IgG (H + L) (ThermoFisher Scientific # A10521) and Cy3-goat anti-rabbit IgG (H + L) (ThermoFisher Scientific # A10520) and counterstaining was achieved with DAPI.

An epifluorescence microscope (AxioImager M2; Zeiss) was used to capture all bright field and immunofluorescence images with an AxioCam ICc5 color camera or an Orca Flash 4.0 sCMOS gray scale camera, respectively. Gray scale immunofluorescence images were false colored using the Zen Pro software (Zeiss).

2.7. Image quantification

To quantify ECM proteins in immunohistochemistry images, entire tubular sections were imaged at 200 × magnification (15−20 images). ImageJ was used to measure the 8-bit pixel intensity of the tissue sections by outlining the tissues and using the "measure" tool in the software [42]. The average pixel intensity values

obtained with ImageJ were inverted (255 minus measured value as 0 represents black and 255 represents white), and averaged for each condition. The average pixel intensity values were additionally normalized over cell density (DAPI staining) to determine the amount of proteins deposited per cell.

2.8. Statistical analysis

Statistical analyses were carried out with the GraphPad Prism 6 or the OriginPro 2017 software. Comparisons among groups were performed by one-way ANOVA with post-hoc Tukey test (to correct for multiple comparisons) for the FN dose-response investigation of disk-shaped sample contraction and compressive E_E, and by two-way ANOVA with post-hoc Tukey test for all other experiments except for immunohistochemistry image analysis for which two tailed *t*-test was employed. Significance was retained when $p < 0.05$. Data are expressed as mean ± standard error of the mean (SEM, $n \geq 4$).

3. Results and discussion

The design and fabrication of biomaterials featuring adequate biological cues to guide cell function is a major challenge in cardiovascular tissue engineering. In particular the scaffold material exerts a major instructive role on embedded cells to deposit and assemble proper ECM networks, which in turn facilitates cell contraction, proliferation, migration and differentiation. Collagen type I is an ideal natural biomaterial for the development of biomimetic scaffolds. Of note, it can be processed to obtain gels that can be readily and uniformly seeded with cells and supplemented during the gel preparation process with some other components such as proteins, peptides or glycosaminoglycans. When SMCs are embedded and cultured within collagen gels they adhere to the substrate and begin contracting the surrounding collagenous matrix in the direction of their axes, thus increasing collagen density and improving construct mechanical properties [47]. In addition, SMCs produce their own ECM and remodel the existing matrix. Directing these processes toward a physiologic-like ECM would be a key step forward in the development of engineered vascular tissue. FN is reported to improve SMC adhesion to 3D scaffolds [48], it can enhance collagen gel contraction by fibroblasts [49], and it plays an important role in the initial phases of elastogenesis [24]. Here, we investigated the usefulness of FN as a master organizer of ECM networks in the static maturation of SMC-cellularised collagen gels, as schematised in the experimental workflow reported in Fig. 1.

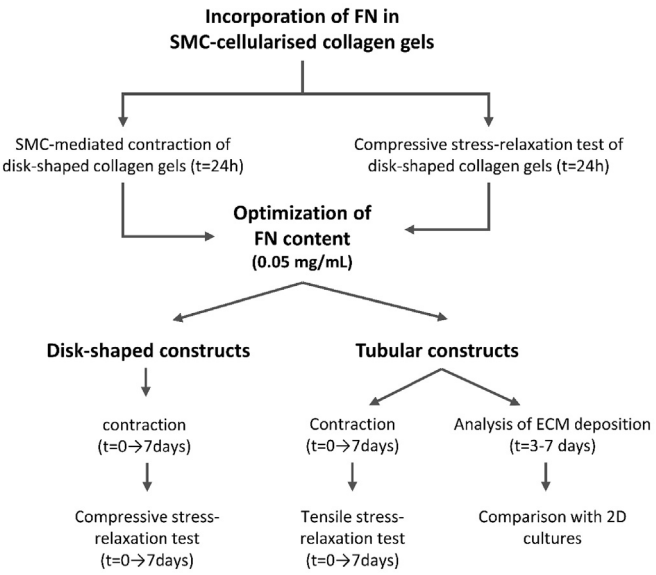

Fig. 1. Schematic overview of experimental workflow.

3.1. Influence of FN on the mechanical properties of disk-shaped SMC-cellularised collagen gels

First, the contraction of disk-shaped SMC-cellularised collagen gels in the presence of different FN concentrations was analysed. As shown in Fig. 2A, FN increased gel contraction after 24 h of culture in a dose-dependent manner, with the maximal contraction (ca 81%) reached for FN concentrations higher than 0.05 mg/mL ($p < 0.05$).

Progressive compression stress-relaxation tests were performed to evaluate the viscoelastic mechanical properties of the disk-shaped SMC-cellularised collagen constructs (Fig. 2B). Since the constructs are composed of collagen type I fibrils of different lengths, cells and interstitial water, multiple relaxation times were expected and the Maxwell-Wiechert model with two Maxwell elements was chosen to analyse stress-relaxation data, as previously reported for collagen [43,50] and other hydrogels [51]. The model (Fig. 2C) can be schematised by a spring with modulus E_E and two Maxwell elements (a spring with modulus E_i and a dashpot with viscosity η_i in series) in parallel and can be described by the following equation:

$$\sigma(t) = \varepsilon_0 \cdot E_E + \varepsilon_0 \cdot E_1 \cdot \exp\left(-\frac{t}{\tau_1}\right) + \varepsilon_0 \cdot E_2 \cdot \exp\left(-\frac{t}{\tau_2}\right)$$

where $\sigma(t)$ is the stress at a given time of each relaxation cycle, ε_0 is the applied strain, E_E is the compressive equilibrium elastic modulus, E_i and τ_i ($i = 1$ to 2) are the elastic components and relaxation times associated to the Maxwell elements, and $\tau_i = \eta_i / E_i$.

The employed Maxwell-Wiechert model provided a robust fit for the stress-relaxation curves, with R^2 values always higher than 0.98. As expected, the compressive E_E of the constructs increased with gel contraction and plateaued for FN concentrations ≥0.05 mg/mL, at values more than two fold higher than plain cellularised collagen gels ($p < 0.05$, Fig. 2D). The presence of FN in collagen gels without SMCs did not influence either contraction (no gel contraction could be observed in the absence of cells after 24 h) or the mechanical properties of the gel (data not shown), suggesting that the effect of FN on the system is mediated by the activity of SMCs, rather than by a direct interaction between FN and the collagen matrix.

The higher contraction mediated by the presence of FN after 24 h culture was confirmed by SEM inspection (Fig. 2E and F) that clearly showed a denser collagen fibrous matrix in presence of FN with respect to plain SMC-cellularised collagen gels.

The remarkable gel contraction is typical of SMC-cellularised collagen gels and leads to a strong time-dependent improvement of the mechanical properties of collagen constructs that, in the absence of cell-mediated contraction, showed a compressive E_E of 0.023 ± 0.05 kPa. On this ground, the effect of maturation under static conditions (up to 7 days) on the properties of the constructs was studied, comparing plain collagen-SMCs constructs (CTRL) with constructs formulated with 0.05 mg/mL FN. Sample contraction continued over the entire time course of the experiment reaching values higher than 90% at 7 days of culture (Fig. 3A). Even if the difference between the two groups progressively diminished, the area of FN-supplemented constructs was always significantly lower than the one of CTRL ($p < 0.05$). At the same time, the

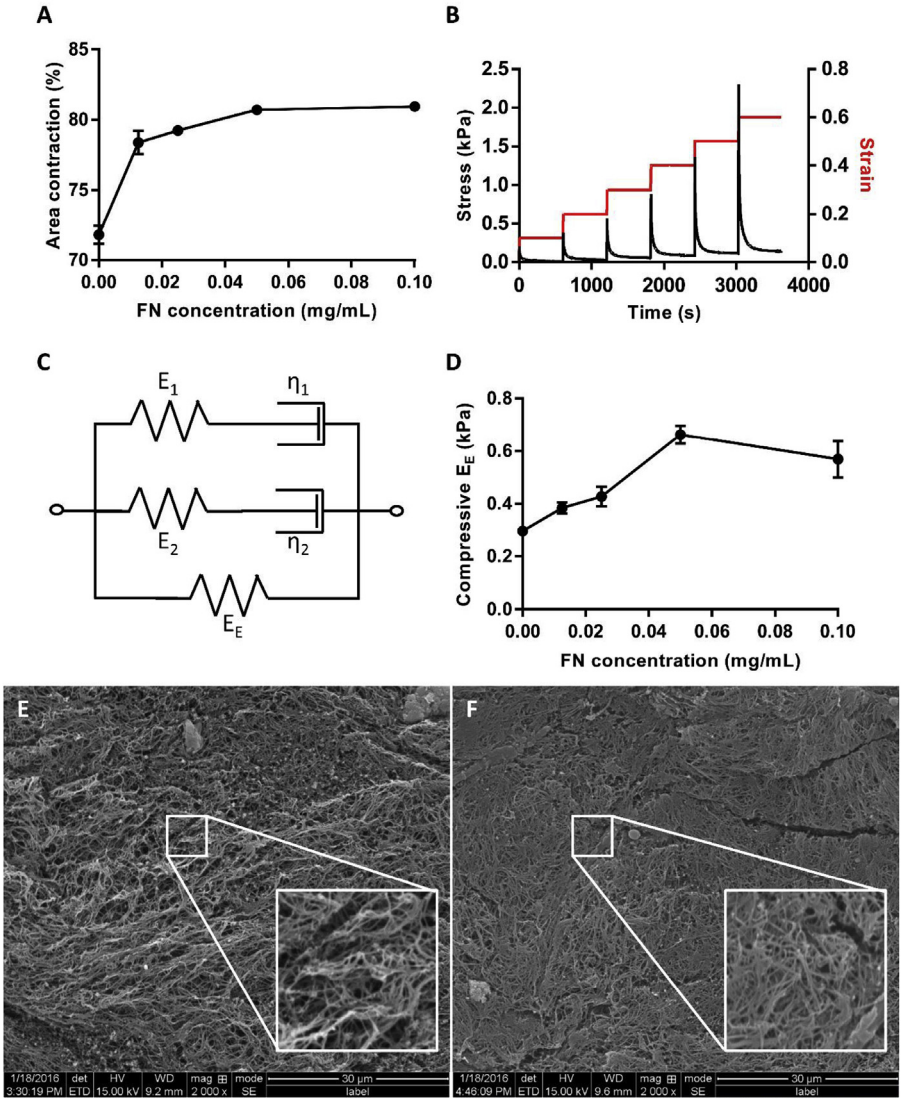

Fig. 2. Consequence of FN on contraction and mechanical properties of disk-shaped collagen constructs cellularised with SMCs. Disk-shaped collagen constructs cellularised with adult porcine aortic smooth muscle cells (PAoSMCs, 5×10^5 cells/mL) were supplemented with the indicated concentrations of plasma FN, cultured for 24 h under static conditions, and then analysed. (A) Dose-response curve of disk-shaped samples contraction. Contraction was evaluated in terms of area reduction with respect to the initial size. (B) Representative typical stress-time (black) and strain-time (red) curves obtained from a progressive compression stress-relaxation test; results from a disk-shaped plain SMC-cellularised collagen gel are reported. (C) Maxwell-Wiechert model with two Maxwell elements used to analyse stress-relaxation data. (D) Dose-response curve of compressive equilibrium elastic modulus (E_E). Compressive E_E was evaluated by progressive stress-relaxation tests under unconfined compression using the Maxwell-Wiechert model with two Maxwell elements. (E) SEM images of SMC-cellularised collagen gels prepared without FN. (F) SEM images of SMC-cellularised collagen gels supplemented with 0.05 mg/mL FN. (SEM images magnification: 2000 ×, inset magnification: 5000 ×). (For interpretation of the references to color in this figure legend, the reader is referred to the Web version of this article.)

compressive E_E strongly increased with time (Fig. 3B), reaching values > 3 kPa after 7 days of culture for the CTRL. Importantly, even after 7 days of maturation, a significantly higher compressive E_E was observed for FN-supplemented constructs with respect to CTRL (about 1.5-fold higher, 0.05 mg/mL FN vs. CTRL, $p < 0.05$).

Cell viability, evaluated by Alamar Blue assay, did not change between CTRL and FN-supplemented gels throughout the experiment ($p > 0.05$, data not shown), suggesting that FN did not alter SMC proliferation that is known to be strongly limited in type I collagen gels [52].

Influence of FN on the mechanical properties of tubular SMC-cellularised collagen gels.

As the blood vessel wall displays a tubular shape and is mainly subjected to circumferential tensile strain due to blood pressure, SMC-cellularised tubular vascular wall models were prepared, using *ad hoc* manufactured moulds, and the influence of FN addition on wall thickness contraction and circumferential tensile mechanical properties was investigated. 0.05 mg/mL FN was used to carry out these experiments based on the optimized properties identified for disk-shaped samples. Tubular models were cultured up to 7 days under static conditions without removing the central mandrel, in order to keep constant the inner diameter of the tubes. As shown in Fig. 4A, a strong contraction of the wall thickness, higher than 80%, was observed already after 24 h of culture, further increasing over time reaching values of about 93% after 7 days. Similarly to disk-shaped samples, a significantly higher contraction was observed for FN-containing gels after 1 and 3 days of maturation ($p < 0.05$), whereas the samples did not differ after 7 days.

The Maxwell-Wiechert model with two Maxwell elements was used again to analyse the data and provided a robust fit for the

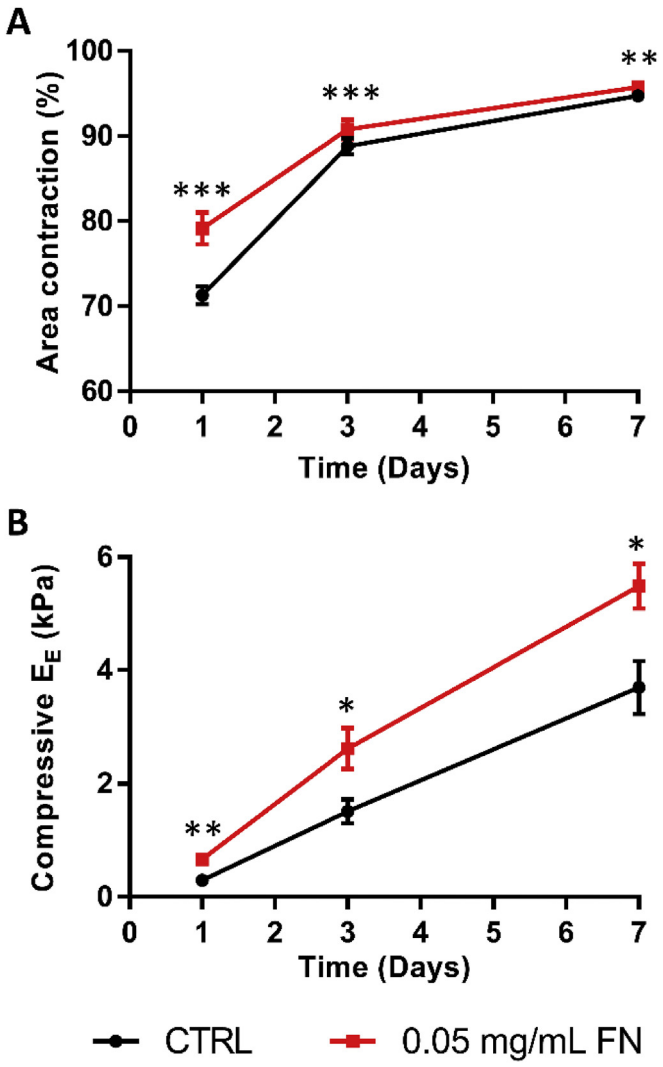

Fig. 3. Time course of (A) gel contraction and (B) compressive equilibrium elastic modulus (E_E) in disk-shaped collagen constructs cellularised with SMCs. The constructs were prepared in the absence (CTRL, black dots) or presence (red squares) of 0.05 mg/mL plasma FN and cultured for 1, 3 and 7 days under static conditions. Contraction was evaluated in terms of area reduction with respect to the disk-shaped gel starting dimensions. Compressive E_E was evaluated by progressive stress-relaxation tests performed under unconfined compression analysed according to Maxwell-Wiechert model with two Maxwell elements. $^{*}p < 0.05$; $^{**}p < 0.01$; $^{***}p < 0.001$, 0.05 mg/mL FN *vs.* CTRL. (For interpretation of the references to color in this figure legend, the reader is referred to the Web version of this article.)

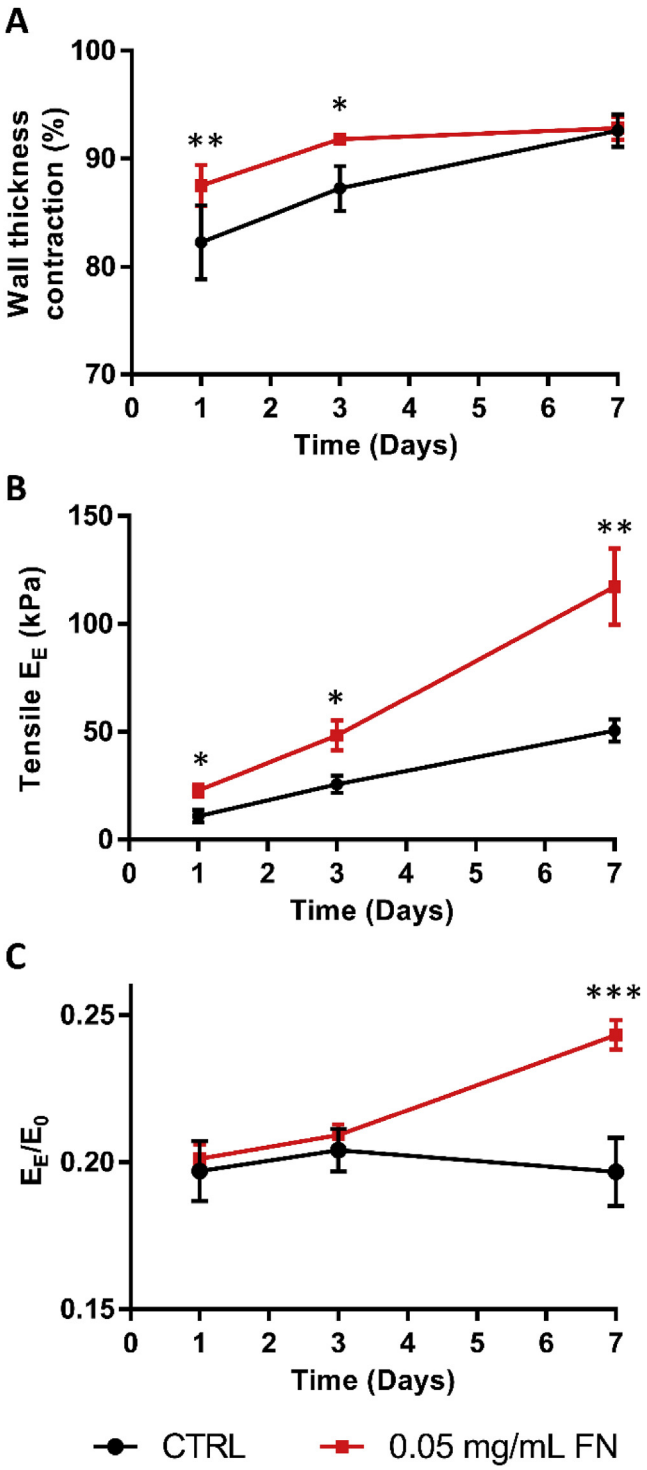

Fig. 4. Time course of (A) contraction, (B) tensile equilibrium elastic modulus (E_E) and (C) ratio of E_E over initial modulus (E_0) in SMC-cellularised tubular collagen constructs. The constructs were prepared in the absence (CTRL, black dots) or presence (red squares) of 0.05 mg/mL plasma FN and cultured for 1, 3 and 7 days under static conditions. Contraction of the tubular constructs was evaluated in terms of wall thickness reduction with respect to the initial tube dimensions. Tensile E_E and E_0 were evaluated by progressive stress-relaxation ring tests analysed according to Maxwell-Wiechert model with two Maxwell elements. $^{*}p < 0.05$; $^{**}p < 0.01$; $^{***}p < 0.001$, 0.05 mg/mL FN *vs.* CTRL. (For interpretation of the references to color in this figure legend, the reader is referred to the Web version of this article.)

stress-relaxation curves, with R^2 values invariably higher than 0.98. Results, reported in Fig. 4B, showed that the tensile E_E increased with the maturation time, from 11 ± 1 kPa at day 1, to 50 ± 3 kPa at day 7 for cellularised gels without FN. Importantly, the presence of FN significantly increased the tensile mechanical properties of the gel, as the tensile E_E increased more than twice in the presence of FN compared to CTRL gels ($p < 0.05$) at every time point.

Interestingly, the elastic modulus obtained after culturing the FN-containing samples for 7 days ($E_E = 117 \pm 18$ kPa) was higher compared to the results reported by Berglund et al. for porcine carotid arteries obtained by similar stress-relaxation tests ($E_E = 50 \pm 12$ kPa) [53] and comparable to values reported for human [54] and porcine [55] coronary arteries (about 100 kPa in both the studies). In addition, the E_E determined in the present study is within the stiffness range or even superior than that of many reported collagen-based scaffolds recently designed to improve

collagen mechanical properties, including chemically cross-linked [56,57], insoluble elastin-supplemented [58], and hyaluronic acid-supplemented [59] porous collagen scaffolds.

The ratio between tensile E_E and the tensile initial (instantaneous) modulus (E_0) was also evaluated. E_0 describes the response of the construct immediately after the application of the strain (defined by stress-strain relationships immediately following the application of the displacement at each step; i.e., $E_0 = E_E + E_1 + E_2$, in the Maxwell-Wiechert model). The E_E/E_0 ratio is an index of the weight of the elastic attributes in the viscoelastic behaviour of the material. Low E_E/E_0 ratios were observed for both, the CTRL and the FN-loaded sample, suggesting a mechanical behaviour dominated by viscous rather than elastic attributes. However, a significant increase in the ratio was observed after 7 days of culture for FN-supplemented gels reaching a value of about 0.24, This is 23%higher compared to constructs without FN ($p < 0.05$) but still lower compared to the value of 0.33 reported for porcine carotid artery [53].

Importantly, the strong increase in the tensile mechanical properties in the presence of FN cannot be ascribed solely to the higher gel contraction and to the consequent increase in collagen density since the size of the constructs at day 7 were comparable in the presence and in the absence of FN. In this light, elastogenic proteins secreted and assembled by SMCs in the constructs were investigated, with the aim to evaluate if FN exerted a role in the deposition of an organised and more elastic ECM with superior mechanical properties.

3.2. Influence of FN on ECM organization and deposition by SMCs

Histological staining by Masson's trichrome showed a uniform distribution of cells within constructs (Fig. 5). As expected, the density of the collagenous matrix increased over time due to the gel contraction and the denser matrix that were observed for FN-supplemented gels at all analysed time points.

To test whether exogenously added plasma FN may alter the deposition of elastic fiber-related proteins produced by SMCs seeded in tubular collagen gel constructs, immunohistochemistry was performed on paraffin sections (Fig. 6A and B). The specimens were stained with antibodies against total FN (plasma and cellular FN), cellular FN (EDA FN), TE, FBN-1, FBN-2, FBLN-4, FBLN-5, LOX, and LTBP-4. The average pixel intensity of the proteins and the average pixel intensity normalized over cell density were plotted (bar graphs in Fig. 6A and B). The increased cell density observed upon exogenous FN addition contributed partially (11.5% at day 3 and 7% at day 7) to the increase of ECM protein deposition/assembly (Fig. 6A and B right bar graphs). As expected, at day 3, constructs matured with supplemental plasma FN showed a significant 2-fold increase in total FN demonstrating that the added plasma FN is retained within the constructs. Endogenously produced cellular FN was also significantly increased by almost 3-fold, albeit at a low base level. FBN-1 and LOX deposition increased modestly at 3 days by about 39 and 30%, respectively, whereas all other tested proteins did change very little (FBN-2, FBLN-4), or not at all (TE, FBLN-5, LTBP-4).

At day 7, plasma FN-matured constructs still retained the added FN, whereas the endogenous cellular FN production was unchanged compared to the controls. Importantly, the deposition of TE was significantly enhanced (53%) after 7 days of culture. Some other critical proteins required for elastic fiber formation were also significantly increased at this time point, including FBN-1 (79%), LOX (44%), and LTBP-4 (63%), whereas the other tested proteins remained unchanged. These results demonstrate that the exogenous addition of plasma FN to tubular SMC-cellularised collagen gels clearly improved the deposition of elastin and other core proteins required for elastic fiber assembly. Increased cell density, in fact, contributed 7−11.5% of the improved ECM deposition.

From the experiments with the cellularised collagen gels, we could not distinguish whether the relevant elastogenic proteins are only deposited into the matrix or indeed assembled into the functional state. To further test whether exogenously added-plasma FN drives the assembly of elastic fibers and related proteins by SMCs, we therefore utilized as proof of principle a 2D SMC culture system that allowed visualization of fibers by immunofluorescence. For this purpose, SMCs were seeded directly on 2D glass slides (in the absence of a 3D collagen scaffold) and analysed through immunofluorescence staining (Fig. 7A and B). The SMCs were cultured for 3 or 7 days in the presence and in the absence of exogenous plasma FN, and stained for total FN (plasma and cellular FN), cellular FN (EDA FN), TE, FBN-1, FBN-2, FBLN-4, FBLN-5, LOX, and LTBP-4. After 3 days of maturation with supplemental plasma FN, both total FN and FBLN-4 showed prominent increases in the number and maturity of fibers, whereas extracellular deposition of the other proteins tested remained unchanged. After 7 days of

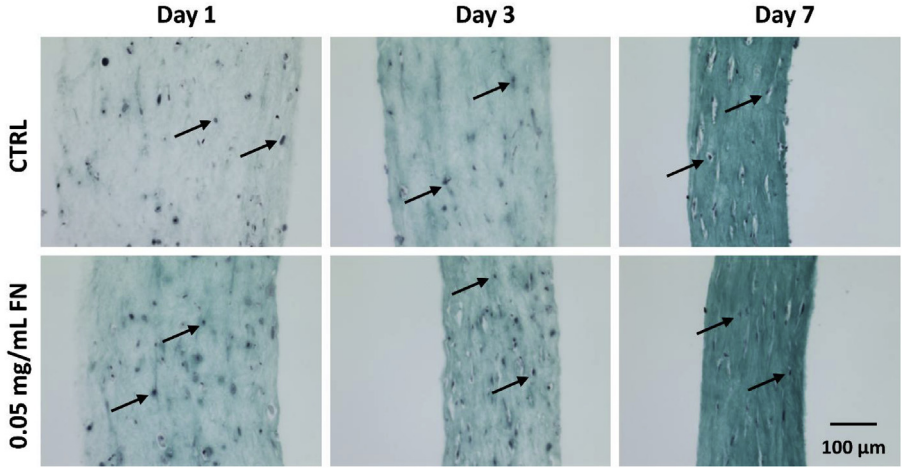

Fig. 5. Histological characterization by Masson's Trichrome staining of tubular collagen constructs cellularised with SMCs. The constructs were prepared in the absence (CTRL) or presence of 0.05 mg/mL plasma FN and cultured for 1, 3 and 7 days under static conditions. 10 µm-thick transversal sections were stained by Masson's Trichrome. The collagenous matrix appears green and the cell nuclei dark purple. Black arrows indicate some of the cells present in the sections. Scale bar: 100 µm for all images. (For interpretation of the references to color in this figure legend, the reader is referred to the Web version of this article.)

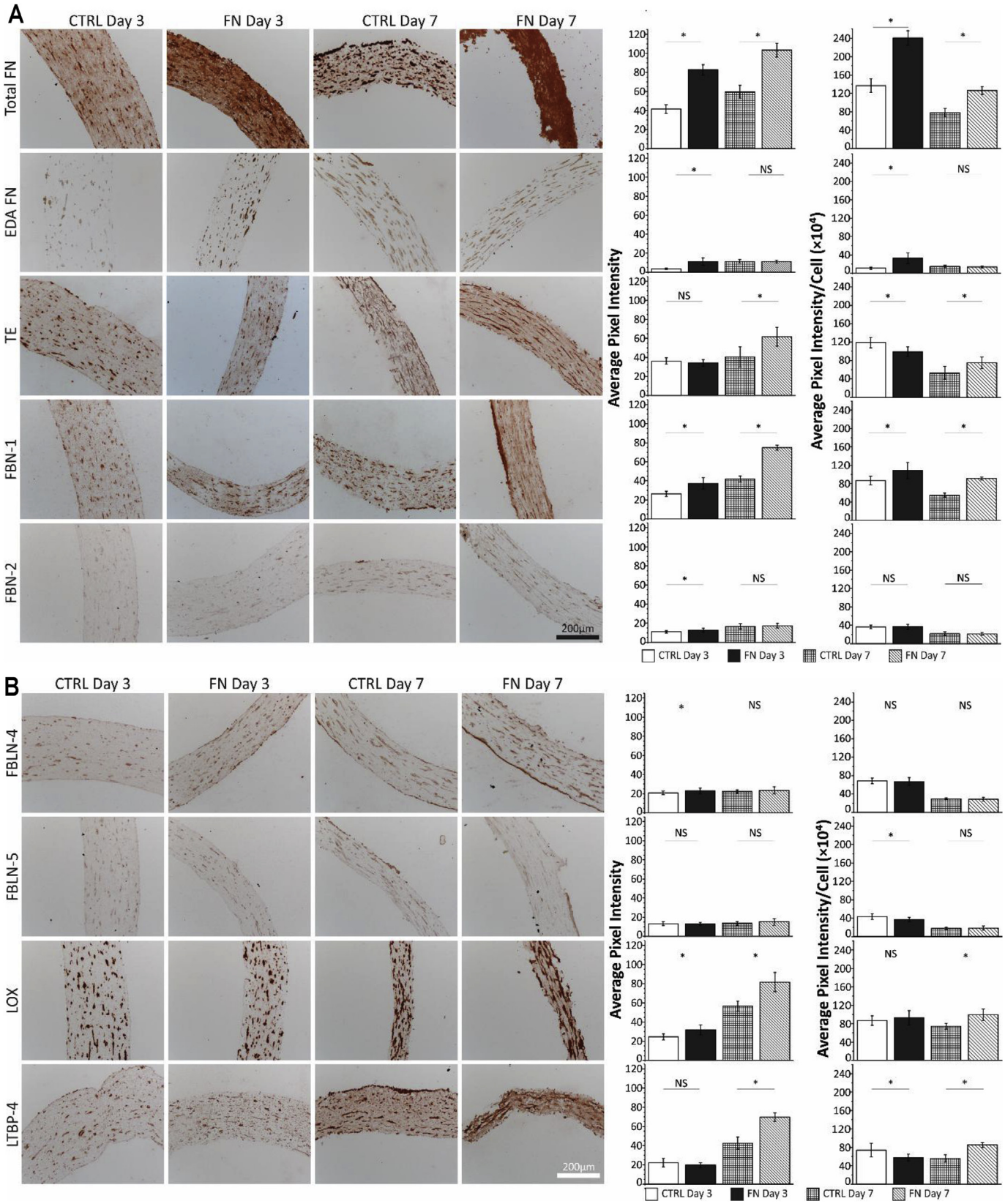

Fig. 6. Immunohistochemical analysis of tubular collagen constructs cellularised with SMCs. Tubular collagen constructs cellularised with PAoSMCs were grown for 3 or 7 days in the absence (CTRL) or presence of exogenously added 0.05 mg/mL plasma FN (FN). The constructs were fixed and stained for critical extracellular matrix proteins associated with elastic fiber formation, including in (A) total fibronectin (total FN), EDA fibronectin (EDA FN), tropoelastin (TE), fibrillin-1 (FBN-1), fibrillin-2 (FBN-2), and in (B) fibulin-4 (FBLN-4), fibulin-5 (FBLN-5), lysyl oxidase (LOX), and latent TGF-β binding protein-4 (LTBP-4). Quantification of the specific signals is shown as Average Pixel Intensity (left bar graphs). The Average Pixel Intensity per cell was determined with DAPI-stained samples (right bar graphs) (*$p < 0.05$, NS = non-significant). Scale bar: 200 µm for all images.

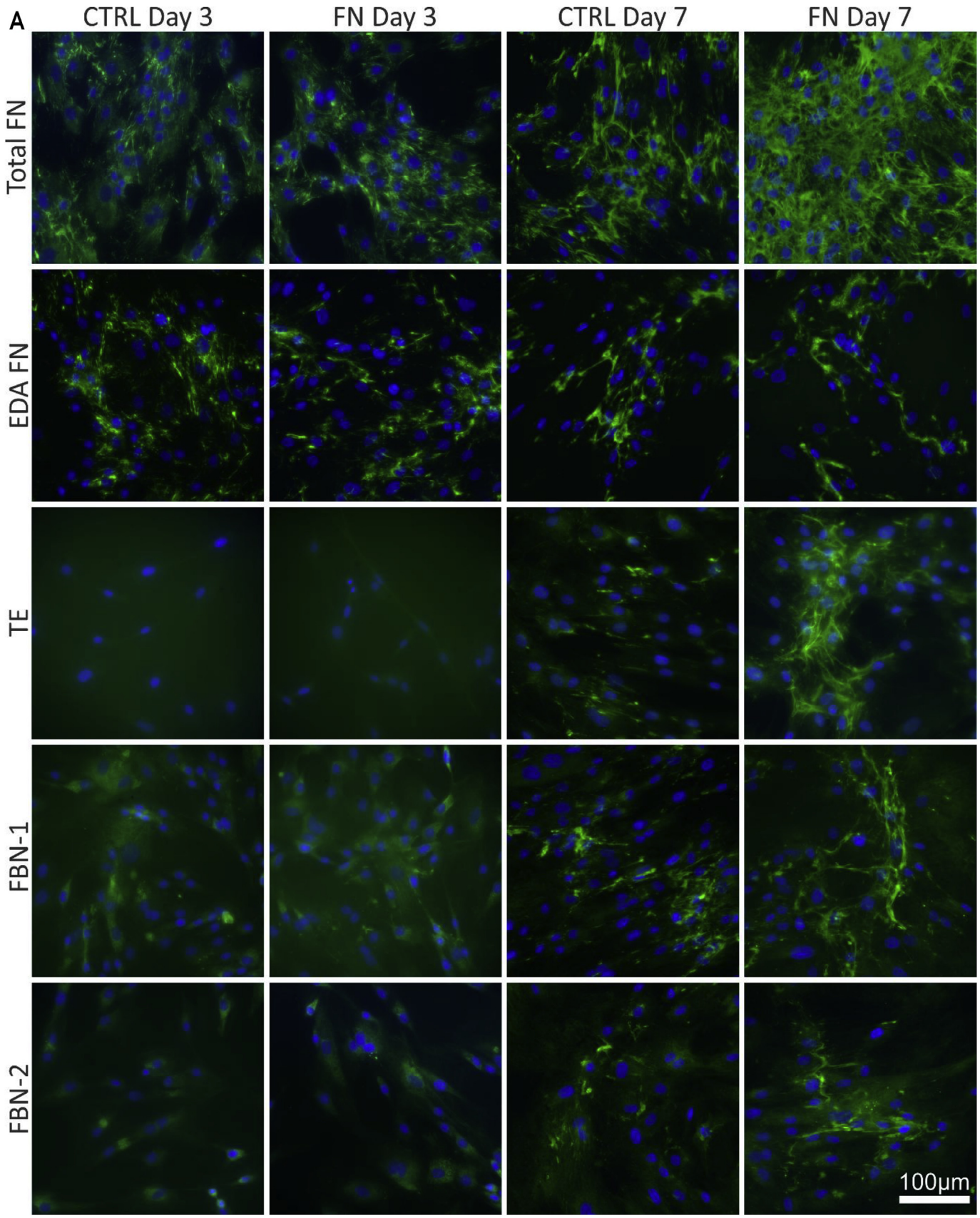

Fig. 7. 2D Immunofluorescence analysis of adult PAoSMCs. Adult PAoSMCs (20,000 per well) were seeded and cultured in 8-well immunofluorescence slides for 3 or 7 days in the absence (CTRL) or presence (FN) of 0.05 mg/mL exogenous plasma FN. After culturing, the cells were fixed and stained for proteins (green signal) associated with elastic fiber formation, including in (A) total fibronectin (Total FN), cellular fibronectin (EDA FN), tropoelastin (TE), fibrillin-1 (FBN-1), fibrillin-2 (FBN-2), and in (B) fibulin-4 (FBLN-4), fibulin-5 (FBLN-5), lysyl oxidase (LOX), and latent TGF-β binding protein-4 (LTBP-4). Cell nuclei are counterstained with DAPI (blue signals). Scale bar: 100 μm for all images. (For interpretation of the references to color in this figure legend, the reader is referred to the Web version of this article.)

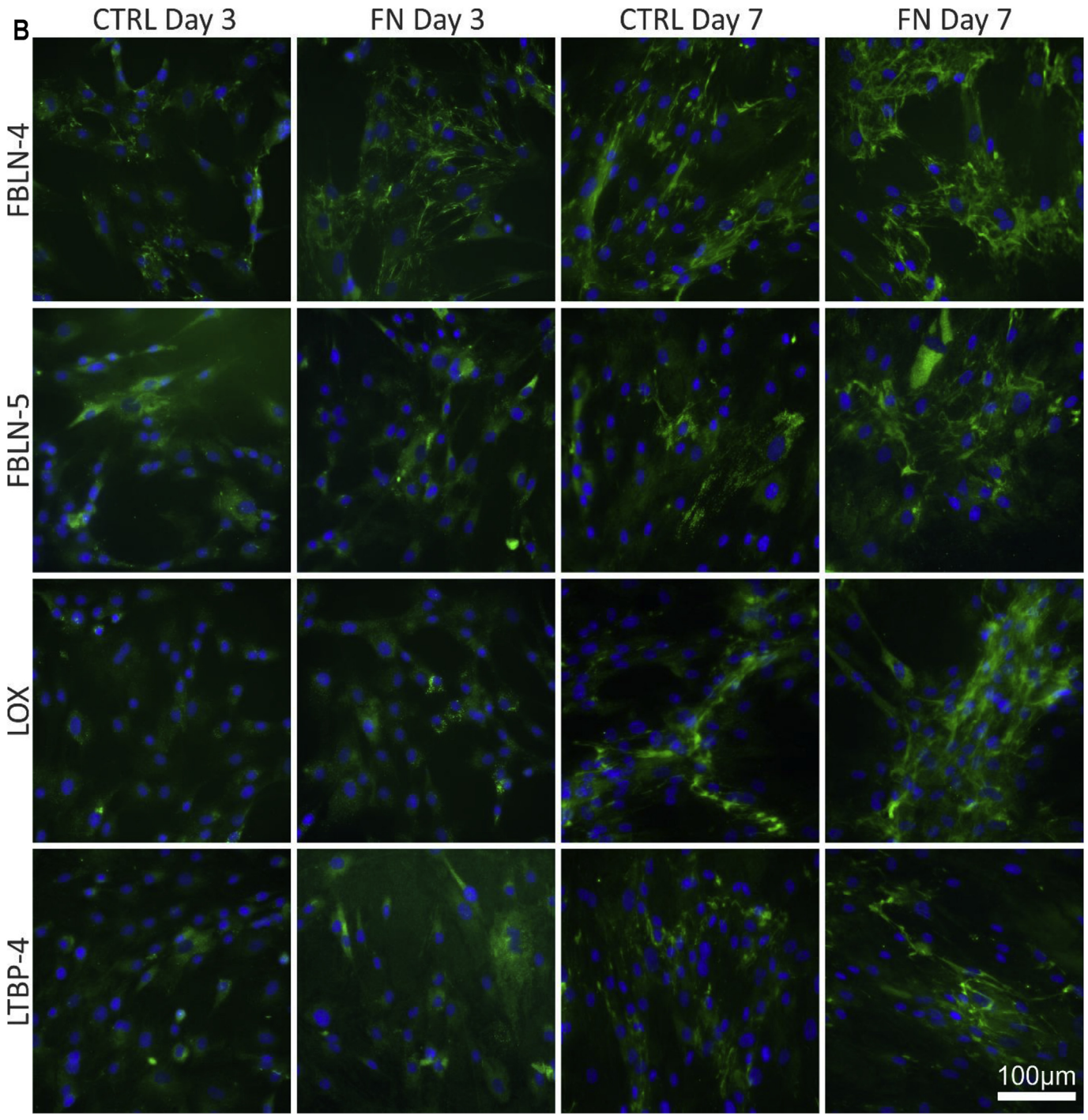

Fig. 7. (*continued*).

SMCs maturation in the presence of supplemental plasma FN, marked increases in the number and maturity of the ECM fibers were observed. Total FN was upregulated whereas cellular FN was not. This demonstrates that the exogenously added plasma FN is integrated over time in the FN network and that it prominently promotes TE fibers deposition, correlating with data obtained with the tubular SMC-cellularised collagen scaffolds. In addition, the presence of all other tested elastogenic proteins in the ECM network was clearly enhanced when SMCs were cultured with plasma FN. Overall, the immunofluorescence data in 2D largely correlated with the results observed with the 3D tubular SMC-cellularised collagen constructs.

In summary, the results on ECM deposition suggest the proposed FN-supplemented SMC-cellularised collagen gel system as a reliable and suitable replacement model for the investigation of elastogenesis occurring in the media layer of blood vessels. It is worthy of note that this process is still not fully understood [22]. Furthermore, the early important deposition of elastic fibers-related proteins in FN-supplemented constructs matured under static conditions is particularly relevant in light of the poor elastic fiber deposition usually observed in 3D engineered vascular tissues where elastin can be observed only after at least 3–4 weeks of

culture [36,37,60].

To provide an overall mechanistic interpretation of the data obtained in this study, it can be speculated that the increase in contraction, mechanical strength and elasticity of the SMC-cellularised collagen constructs supplemented with FN is likely mediated by the specific roles that FN exerts in promoting cell interaction and matrix assembly. FN interacts with cells via integrin $\alpha5\beta1$ and $\alpha v\beta3$ through the conserved RGD sequence located on the 10th FN type III domain [61]. Integrins serve as linkers connecting FN to the actin cytoskeleton, the main machinery for SMC contraction [62,63]. In addition, Sun et al., using atomic force microscopy to apply forces to specific ECM adhesion sites on SMCs, have shown that FN features a unique ability to strongly interact with SMCs, forming $\alpha5\beta1$-and $\alpha v\beta3$-rich focal adhesions that are mechanically active and stimulate cell contraction [64]. FN also binds to collagen, being required for its polymerization and assembly [65,66]. The binding site for collagen on FN is located in an N-terminal region in some distance to the RGD cell binding site [67]. This positions the FN supplemented in the 3D SMC-cellularised collagen constructs as a bridge which binds to the cells and the actin cytoskeleton through its centrally located RGD sequence and to collagen type I in the gels via the N-terminus. Therefore, these FN-bridges can increase the number of cell adhesion points to collagen and activate cell contraction, finally speeding up construct compaction. This hypothesis is in agreement with the study by Hocking et al., who observed that FN stimulates the spreading of FN-null embryo cells on collagen fibrils, triggering an increase in contractility and in collagen contraction [68]. We speculate that the presence of properly assembled collagen type I fibers together with the increased gel compaction mediated by contracting SMCs, could account for the increased mechanical properties of the FN-substituted collagen gels.

FN also facilitates the assembly of FBN-1 into microfibrils [24,25], providing an essential scaffold for the deposition of tropoelastin [22], which in turn requires LTBP-4 [28]. The presence of fully developed elastic fibers would explain the enhanced elastic properties of the FN-supplemented cellularised constructs. These claims are further supported by the increased LOX levels found in FN-substituted collagen gels. LOX, in fact, is the extracellular cross-linking enzyme for both collagen and elastic fibers [69], which provides them with the required stability and elasticity.

4. Conclusions

In this study soluble plasma FN was added to SMC-cellularised collagen gels in order to improve the maturation of the resulting engineered vascular wall models. The optimized FN concentration of 0.05 mg/mL led to a faster contraction of the collagen matrix and to enhanced mechanical compression and tension properties, combined with an increase in elasticity. The ECM remodeling and deposition mediated by SMCs in the presence of FN resulted in a denser collagen matrix enriched in elastic fibers and associated with enhanced elastogenic FBN-1, LOX and LTBP-4 networks. The data show that elastogenesis is effectively undergoing in the constructs. Altogether, these results demonstrate that exogenously added FN, a recognised master organizer of the ECM, exerts pivotal roles in directing the remodeling of scaffolds by SMCs toward the production of a physiological-like, elastic fiber-containing ECM. This approach may prove very useful in the generation of mature, physiologically relevant vessel wall models that are well suited for the development and preclinical testing of drugs and vascular devices, or to study physiological processes such as elastogenesis. FN-supplemented SMC-cellularised collagen constructs could also be regarded as a step forward toward functional TEBVs, although further in-depth studies especially on longitudinal, circumferential and radial mechanical properties and on suturability are needed. FN addition might also be considered for other soft or connective tissue applications, such as engineered skin, lung tissues, ligaments, and tendons, whenever the generation of mature tissues with elastic or viscoelastic behaviour is desired.

Acknowledgements

We thank Jiongci Xu for excellent help with image quantifications. DP was awarded a post-doctoral scholarship from the NSERC CREATE Program in Regenerative Medicine. This work was supported by operating grants from the Fonds de Recherche du Québec - Nature et Technologies (FWO-Quebec collaborative project, and Team Research Project), the Natural Sciences and Engineering Research Council of Canada (DM and DPR), the Heart and Stroke Foundation of Canada (HSFC G-16-00014634, DPR), the Quebec Network for Oral and Bone Health Research, the CHU de Québec, and the Canada Research Chair program (DM and DPR).

Appendix A. Supplementary data

Supplementary data related to this article can be found at https://doi.org/10.1016/j.biomaterials.2018.07.013.

Declarations of interest

None.

Conflicts of interest

The authors confirm that there are no known conflicts of interest associated with this publication and there has been no significant financial support for this work that could have influenced its outcome.

Data availability

The raw/processed data required to reproduce these findings cannot be shared at this time due to technical or time limitations. Data will be made available on request.

References

[1] D. Mozaffarian, E.J. Benjamin, A.S. Go, D.K. Arnett, M.J. Blaha, M. Cushman, S. de Ferranti, J.-P. Despres, H.J. Fullerton, V.J. Howard, M.D. Huffman, S.E. Judd, B.M. Kissela, D.T. Lackland, J.H. Lichtman, L.D. Lisabeth, S. Liu, R.H. Mackey, D.B. Matchar, D.K. McGuire, E.R. Mohler III, C.S. Moy, P. Muntner, M.E. Mussolino, K. Nasir, R.W. Neumar, G. Nichol, L. Palaniappan, D.K. Pandey, M.J. Reeves, C.J. Rodriguez, P.D. Sorlie, J. Stein, A. Towfighi, T.N. Turan, S.S. Virani, J.Z. Willey, D. Woo, R.W. Yeh, M.B. Turner, C. Amer Heart Assoc Stat, S. Stroke Stat, Executive summary: Heart disease and Stroke Statistics-2015 update a report from the american Heart association, Circulation 131 (4)(2015) 434–441.

[2] L. Shan, A. Saxena, R. McMahon, A. Newcomb, Coronary artery bypass graft surgery in the elderly a review of postoperative quality of life, Circulation 128 (21) (2013) 2333–2343.

[3] D. Pezzoli, E. Cauli, P. Chevallier, S. Fare, D. Mantovani, Biomimetic coating of cross-linked gelatin to improve mechanical and biological properties of electrospun PET: a promising approach for small caliber vascular graft applications, J. Biomed. Mater. Res. 105 (9) (2017) 2405–2415.

[4] M.C. Gibbons, M.A. Foley, K.O.H. Cardinal, Thinking inside the box: keeping tissue-engineered constructs in vitro for use as preclinical models, Tissue Eng. B Rev. 19 (1) (2013) 14–30.

[5] A. Holmes, R. Brown, K. Shakesheff, Engineering tissue alternatives to animals: applying tissue engineering to basic research and safety testing, Regen. Med. 4 (4) (2009) 579–592.

[6] N. Rajan, J. Habermehl, M.-F. Cote, C.J. Doillon, D. Mantovani, Preparation of ready-to-use, storable and reconstituted type I collagen from rat tail tendon for tissue engineering applications, Nat. Protoc. 1 (6) (2007) 2753–2758.

[7] D.G. Seifu, A. Purnama, K. Mequanint, D. Mantovani, Small-diameter vascular tissue engineering, Nat. Rev. Cardiol. 10 (7) (2013) 410–421.

[8] C.B. Weinberg, E. Bell, A blood vessel model constructed from collagen and cultured vascular cells, Science 231 (4736) (1986) 397–400.
[9] K. Bilodeau, F. Couet, F. Boccafoschi, D. Mantovani, Design of a perfusion bioreactor specific to the regeneration of vascular tissues under mechanical stresses, Artif. Organs 29 (11) (2005) 906–912.
[10] F. Boccafoschi, N. Rajan, J. Habermehl, D. Mantovani, Preparation and characterization of a scaffold for vascular tissue engineering by direct-assembling of collagen and cells in a cylindrical geometry, Macromol. Biosci. 7 (5) (2007) 719–726.
[11] S. Meghezi, D.G. Seifu, N. Bono, L. Unsworth, K. Mequanint, D. Mantovani, Engineering 3D cellularized collagen gels for vascular tissue regeneration, J. Visual. Exp. 100 (2015), e52812.
[12] L. Lévesque, C. Loy, A. Lainé, B. Drouin, P. Chevallier, D. Mantovani, Incrementing the frequency of dynamic strain on SMC-cellularised collagen-based scaffolds affects extracellular matrix remodeling and mechanical properties, ACS Biomater. Sci. Eng. (2017), https://doi.org/10.1021/acsbiomaterials.7b00395. In Press.
[13] C. Loy, S. Meghezi, L. Levesque, D. Pezzoli, H. Kumra, D. Reinhardt, J.N. Kizhakkedathu, D. Mantovani, A planar model of the vessel wall from cellularized-collagen scaffolds: focus on cell-matrix interactions in mono-,bi- and tri-culture models, Biomater. Sci. 5 (1) (2017) 153–162.
[14] C. Loy, D. Pezzoli, G. Candiani, D. Mantovani, A cost-effective culture system for the in vitro assembly, maturation, and stimulation of advanced multilayered multiculture tubular tissue models, Biotechnol. J. (2017), 1700359, https://doi.org/10.1002/biot.201700359.
[15] N. Bono, S. Meghezi, M. Soncini, M. Piola, D. Mantovani, G.B. Fiore, A dual-mode bioreactor system for tissue engineered vascular models, Ann. Biomed. Eng. 45 (6) (2017) 1496–1510.
[16] M. Achilli, D. Mantovani, Tailoring mechanical properties of collagen-based scaffolds for vascular tissue engineering: the effects of pH, temperature and ionic strength on gelation, Polymers 2 (4) (2010) 664–680.
[17] E.A. Abou Neel, U. Cheema, J.C. Knowles, R.A. Brown, S.N. Nazhat, Use of multiple unconfined compression for control of collagen gel scaffold density and mechanical properties, Soft Matter 2 (11) (2006) 986–992.
[18] C.E. Ghezzi, B. Marelli, N. Muja, S.N. Nazhat, Immediate production of a tubular dense collagen construct with bioinspired mechanical properties, Acta Biomater. 8 (5) (2012) 1813–1825.
[19] H.Y. Tuan-Mu, P.C. Lu, P.Y. Lee, C.C. Lin, C.J. Chen, L.L.H. Huang, J.H. Lin, J.J. Hu, Rapid fabrication of a cell-seeded collagen gel-based tubular construct that withstands arterial pressure, Ann. Biomed. Eng. 44 (11) (2016) 3384–3397.
[20] A.K. Baldwin, A. Simpson, R. Steer, S.A. Cain, C.M. Kielty, Elastic fibres in health and disease, Expet Rev. Mol. Med. 15 (2013) e8.
[21] J.E. Wagenseil, R.P. Mecham, Vascular extracellular matrix and arterial mechanics, Physiol. Rev. 89 (3) (2009) 957–989.
[22] J.E. Wagenseil, R.P. Mecham, New insights into elastic fiber assembly, Birth Def. Res. C 81 (4) (2007) 229–240.
[23] P. Singh, C. Carraher, J.E. Schwarzbauer, Assembly of fibronectin extracellular matrix, Annu. Rev. Cell Dev. Biol. 26 (2010) 397–419.
[24] L. Sabatier, D. Chen, C. Fagotto-Kaufmann, D. Hubmacher, M.D. McKee, D.S. Annis, D.F. Mosher, D.P. Reinhardt, Fibrillin assembly requires fibronectin, Mol. Biol. Cell 20 (3) (2009) 846–858.
[25] R. Kinsey, M.R. Williamson, S. Chaudhry, K.T. Mellody, A. McGovern, S. Takahashi, C.A. Shuttleworth, C.M. Kielty, Fibrillin-1 microfibril deposition is dependent on fibronectin assembly, J. Cell Sci. 121 (16) (2008) 2696–2704.
[26] J. Sottile, D.C. Hocking, Fibronectin polymerization regulates the composition and stability of extracellular matrix fibrils and cell-matrix adhesions, Mol. Biol. Cell 13 (10) (2002) 3546–3559.
[27] C.L. Papke, H. Yanagisawa, Fibulin-4 and fibulin-5 in elastogenesis and beyond: insights from mouse and human studies, Matrix Biol. 37 (2014) 142–149.
[28] K. Noda, B. Dabovic, K. Takagi, T. Inoue, M. Horiguchi, M. Hirai, Y. Fujikawa, T.O. Akama, K. Kusumoto, L. Zilberberg, L.Y. Sakai, K. Koli, M. Naitoh, H. von Melchner, S. Suzuki, D.B. Rifkin, T. Nakamura, Latent TGF-beta binding protein 4 promotes elastic fiber assembly by interacting with fibulin-5, Proc. Natl. Acad. Sci. U. S. A. 110 (8) (2013) 2852–2857.
[29] M. Horiguchi, T. Inoue, T. Ohbayashi, M. Hirai, K. Noda, L.Y. Marmorstein, D. Yabe, K. Takagi, T.O. Akama, T. Kita, T. Kimura, T. Nakamura, Fibulin-4 conducts proper elastogenesis via interaction with cross-linking enzyme lysyl oxidase, Proc. Natl. Acad. Sci. U. S. A. 106 (45) (2009) 19029–19034.
[30] X.Q. Liu, Y. Zhao, J.G. Gao, B. Pawlyk, B. Starcher, J.A. Spencer, H. Yanagisawa, J. Zuo, T.S. Li, Elastic fiber homeostasis requires lysyl oxidase-like 1 protein, Nat. Genet. 36 (2) (2004) 178–182.
[31] A. Patel, B. Fine, M. Sandig, K. Mequanint, Elastin biosynthesis: the missing link in tissue-engineered blood vessels, Cardiovasc. Res. 71 (1) (2006) 40–49.
[32] G. Dubey, K. Mequanint, Conjugation of fibronectin onto three-dimensional porous scaffolds for vascular tissue engineering applications, Acta Biomater. 7 (3) (2011) 1114–1125.
[33] F. Shi, X.C. Long, A. Hendershot, J.M. Miano, J. Sottile, Fibronectin matrix polymerization regulates smooth muscle cell phenotype through a Rac1 dependent mechanism, PLoS One 9 (4) (2014), e94988.
[34] D.Y. Li, B. Brooke, E.C. Davis, R.P. Mecham, L.K. Sorensen, B.B. Boak, E. Eichwald, M.T. Keating, Elastin is an essential determinant of arterial morphogenesis, Nature 393 (6682) (1998) 276–280.
[35] S.G. Wise, G.C. Yeo, M.A. Hiob, J. Rnjak-Kovacina, D.L. Kaplan, M.K.C. Ng, A.S. Weiss, Tropoelastin: a versatile, bioactive assembly module, Acta Biomater. 10 (4) (2014) 1532–1541.
[36] J.L. Long, R.T. Tranquillo, Elastic fiber production in cardiovascular tissue-equivalents, Matrix Biol. 22 (4) (2003) 339–350.
[37] L. Venkataraman, C.A. Bashur, A. Ramamurthi, Impact of cyclic stretch on induced elastogenesis within collagenous conduits, Tissue Eng. 20 (9–10) (2014) 1403–1415.
[38] K.-W. Lee, D.B. Stolz, Y. Wang, Substantial expression of mature elastin in arterial constructs, Proc. Natl. Acad. Sci. U. S. A. 108 (7) (2011) 2705–2710.
[39] S. Hinderer, N. Shen, L.-J. Ringuette, J. Hansmann, D.P. Reinhardt, S.Y. Brucker, E.C. Davis, K. Schenke-Layland, In vitro elastogenesis: instructing human vascular smooth muscle cells to generate an elastic fiber-containing extracellular matrix scaffold, Biomed. Mater. 10 (3) (2015) 034102.
[40] D. Pezzoli, E.K. Tsekoura, K.C. Remant Bahadur, G. Candiani, D. Mantovani, H. Uludağ, Hydrophobe-substituted bPEI derivatives: boosting transfection on primary vascular cells, Sci. China Mater. 60 (6) (2017) 529–542.
[41] N. Bono, D. Pezzoli, L. Levesque, C. Loy, G. Candiani, G.B. Fiore, D. Mantovani, Unraveling the role of mechanical stimulation on smooth muscle cells: a comparative study between 2D and 3D models, Biotechnol. Bioeng. 113 (10) (2016) 2254–2263.
[42] C.A. Schneider, W.S. Rasband, K.W. Eliceiri, NIH Image to ImageJ: 25 years of image analysis, Nat. Methods 9 (7) (2012) 671–675.
[43] S. Meghezi, F. Couet, P. Chevallier, D. Mantovani, Effects of a pseudophysiological environment on the elastic and viscoelastic properties of collagen gels, Int. J. Biomater. 2012 (2012) 319290.
[44] E. El-Hallous, T. Sasaki, D. Hubmacher, M. Getie, K. Tiedemann, J. Brinckmann, B. Batge, E.C. Davis, D.P. Reinhardt, Fibrillin-1 interactions with fibulins depend on the first hybrid domain and provide an adaptor function to tropoelastin, J. Biol. Chem. 282 (12) (2007) 8935–8946.
[45] K. Tiedemann, B. Batge, P.K. Muller, D.P. Reinhardt, Interactions of fibrillin-1 with heparin/heparan sulfate, implications for microfibrillar assembly, J. Biol. Chem. 276 (38) (2001) 36035–36042.
[46] E.G. Hayman, E. Ruoslahti, Distribution of fetal bovine serum fibronectin and endogenous rat cell fibronectin in extracellular matrix, J. Cell Biol. 83 (1)(1979) 255–259.
[47] L. Amadori, N. Rajan, S. Vesentini, D. Mantovani, Atomic force and confocal microscopic studies of collagen-cell-based scaffolds for vascular tissue engineering, Adv. Mater. Res. 15–17 (2007) 83–88.
[48] S.G. Lin, M. Sandig, K. Mequanint, Three-Dimensional topography of synthetic scaffolds induces elastin synthesis by human coronary artery smooth muscle cells, Tissue Eng. 17 (11–12) (2011) 1561–1571.
[49] Y. Liu, R. Yanai, Y. Lu, K. Kimura, T. Nishida, Promotion by fibronectin of collagen gel contraction mediated by human corneal fibroblasts, Exp. Eye Res. 83 (5) (2006) 1196–1204.
[50] Z.L.L. Shen, H. Kahn, R. Ballarin, S.J. Eppell, Viscoelastic properties of isolated collagen fibrils, Biophys. J. 100 (12) (2011) 3008–3015.
[51] J.D. Kaufman, G.J. Miller, E.F. Morgan, C.M. Klapperich, Time-dependent mechanical characterization of poly(2-hydroxyethyl methacrylate) hydrogels using nanoindentation and unconfined compression, J. Mater. Res. 23 (5) (2008) 1472–1481.
[52] A.L. Plant, K. Bhadriraju, T.A. Spurlin, J.T. Elliott, Cell response to matrix mechanics: focus on collagen, Biochim. Biophys. Acta Mol. Cell Res. 1793 (5) (2009) 893–902.
[53] J.D. Berglund, R.M. Nerem, A. Sambanis, Viscoelastic testing methodologies for tissue engineered blood vessels, J. Biomech. Eng. 127 (7) (2005) 1176–1184.
[54] M.H. Kural, M. Cai, D. Tang, T. Gwyther, J. Zheng, K.L. Billiar, Planar biaxial characterization of diseased human coronary and carotid arteries for computational modeling, J. Biomech. 45 (5) (2012) 790–798.
[55] M. Garcia, G.S. Kassab, Right coronary artery becomes stiffer with increase in elastin and collagen in right ventricular hypertrophy, J. Appl. Physiol. 106 (4) (2009) 1338–1346.
[56] C.N. Grover, R.E. Cameron, S.M. Best, Investigating the morphological, mechanical and degradation properties of scaffolds comprising collagen, gelatin and elastin for use in soft tissue engineering, J. Mech. Behav. Biomed. Mater. 10 (2012) 62–74.
[57] N. Guoguang, C. Tracy, S. Etai, L. Sang-Jin, S. Shay, The influence of cross-linking methods on the mechanical and biocompatible properties of vascular scaffold, J. Sci. Appl.: Biomed. 1 (1) (2013) 1–7.
[58] A.J. Ryan, F.J. O'Brien, Insoluble elastin reduces collagen scaffold stiffness, improves viscoelastic properties, and induces a contractile phenotype in smooth muscle cells, Biomaterials 73 (2015) 296–307.
[59] C. Zhu, D. Fan, Y. Wang, Human-like collagen/hyaluronic acid 3D scaffolds for vascular tissue engineering, Mater. Sci. Eng. C 34 (2014) 393–401.
[60] L. Venkataraman, A. Ramamurthi, Induced elastic matrix deposition within three-dimensional collagen scaffolds, Tissue Eng. 17 (21–22) (2011) 2879–2889.
[61] E.H.J. Danen, P. Sonneveld, C. Brakebusch, R. Fassler, A. Sonnenberg, The fibronectin-binding integrins alpha 5 beta 1 and alpha v beta 3 differentially modulate RhoA-GTP loading, organization of cell matrix adhesions, and fibronectin fibrillogenesis, J. Cell Biol. 159 (6) (2002) 1071–1086.
[62] J.W. Tamkun, D.W. Desimone, D. Fonda, R.S. Patel, C. Buck, A.F. Horwitz, R.O. Hynes, Structure of integrin, a glycoprotein involved in the trans-membrane linkage between fibronectin and actin, Cell 46 (2) (1986) 271–282.
[63] Q.H. Zhang, M.K. Magnusson, D.F. Mosher, Lysophosphatidic acid and microtubule-destabilizing agents stimulate fibronectin matrix assembly through Rho-dependent actin stress fiber formation and cell contraction, Mol.

Biol. Cell 8 (8) (1997) 1415–1425.
[64] Z. Sun, L.A. Martinez-Lemus, M.A. Hill, G.A. Meininger, Extracellular matrix-specific focal adhesions in vascular smooth muscle produce mechanically active adhesion sites, Am. J. Physiol. Cell Physiol. 295 (1) (2008) C268–C278.
[65] T. Velling, J. Risteli, K. Wennerberg, D.F. Mosher, S. Johansson, Polymerization of type I and III collagens is dependent on fibronectin and enhanced by integrins alpha(11)beta(1) and alpha(2)beta(1), J. Biol. Chem. 277 (40) (2002) 37377–37381.
[66] S.H. Li, C. Van den Diepstraten, S.J. D'Souza, B.M.C. Chan, J.G. Pickering, Vascular smooth muscle cells orchestrate the assembly of type I collagen via alpha 2 beta 1 integrin, RhoA, and fibronectin polymerization, Am. J. Pathol. 163 (3) (2003) 1045–1056.
[67] R.J. Owens, F.E. Baralle, Mapping the collagen-binding site of human fibronectin by expression in escherichia-coli, EMBO J. 5 (11) (1986) 2825–2830.
[68] D.C. Hocking, J. Sottile, K.J. Langenbach, Stimulation of integrin-mediated cell contractility by fibronectin polymerization, J. Biol. Chem. 275 (14) (2000) 10673–10682.
[69] L.I. Smith-Mungo, H.M. Kagan, Lysyl oxidase: properties, regulation and multiple functions in biology, Matrix Biol. 16 (7) (1998) 387–398.